JOURNAL OF GEOPHYSICAL RESEARCH, VOL. 103, NO. D23, PAGES 31,241–31,254, DECEMBER 20, 1998

Enhanced absorption of UV radiation due to multiple scattering in clouds: Experimental evidence and theoretical explanation

B. Mayer,[1,5] A. Kylling,[2,3] S. Madronich,[1] and G. Seckmeyer[4]

Abstract. Measurements of spectral ultraviolet-B irradiance under optically thick clouds show strongly enhanced attenuation by molecular and particulate absorbers. The atmospheric photon path is enhanced owing to the presence of a highly scattering medium, leading to an amplification of absorption by tropospheric ozone and aerosol. Calculations with discrete ordinate and Monte Carlo models show that photon paths in realistic water clouds may be enhanced by factors of 10 and more compared to cloudless sky. Model calculations further show that UV spectra measured under thick clouds can be well simulated within 10%, indicating that the involved processes are quantitatively described by current models. These findings are of important consequence for all ground-based remote sensing applications which take advantage of measuring scattered radiation in order to infer atmospheric trace gas abundances. These algorithms, for example, the calculation of total ozone from global irradiance or zenith sky radiance, are subject to large errors, when neglecting the influence of cloud scattering on the derived data. In the present study, errors of more than 300 Dobson Units (DU) have been found, if such methods were applied without care in the presence of thick clouds.

1. Introduction

Attenuation of ultraviolet radiation by clouds is often considered to be independent of wavelength [e.g., *Webb,* 1992; *Frederick et al.,* 1993]. Although the main optical properties of water clouds, the extinction coefficient, the single-scattering albedo, and the asymmetry factor, are in fact nearly constant with wavelength in the UV range [*Hu and Stamnes*, 1993], the combination of cloud scattering with other, wavelength-dependent atmospheric processes has been demonstrated to introduce a wavelength dependence into the cloud attenuation. *Frederick and Lubin* [1988] and *Wang and Lenoble* [1996] showed with their calculations that cloud transmittance, which is defined as the ratio of the irradiance in presence of a cloud and the corresponding cloudless sky irradiance, peaks between 320 and 330 nm and decreases toward longer and shorter wavelengths. *Seckmeyer et al.* [1996b] and *Kylling et al.* [1997] presented and interpreted measurements under a thin cloud, demonstrating that cloud scattering in combination with Rayleigh scattering may result in a distinct wavelength dependence of the cloud transmittance. Here we show that coupling of cloud scattering and molecular or particulate absorption can result in a strong enhancement of absorption which appears as a pronounced wavelength dependence of cloud attenuation. Without knowledge of the underlying physics, such observation is easily misinterpreted as too high amounts of the absorber.

One manifestation of this phenomenon is the so-called "cumulus effect," an abnormal increase of the inferred total ozone during heavily clouded skies. When the direct Sun is not visible, total ozone is derived from zenith sky or global irradiance measurements at two or more wavelengths, for example, the Dobson wavelength pairs. *Dobson and Norman* [1957] already reported an increase of the zenith-derived total ozone of up to 200 DU during heavily clouded sky, which he referred to as the cumulus effect. A similar effect was reported by *Brewer and Kerr* [1973], *Mayer and Seckmeyer* [1996], and *Fioletov et al.* [1997]. *Erle et al.* [1995] observed an increase in the total ozone, derived from zenith sky differential optical absorption spectroscopy (DOAS) measurements, which they explained by tropospheric light path enhancement: Because of scattering in a cloud, the tropospheric light path was enhanced by a factor of up to 10, leading to an error of up to 10–30% in the derived

[1]National Center for Atmospheric Research (NCAR), Boulder, Colorado.
[2]Norwegian Institute for Air Research (NILU), Tromsø, Norway.
[3]Also at Geophysical Institute, University of Oslo, Norway.
[4]Fraunhofer Institute for Atmospheric Environmental Research (IFU), Garmisch–Partenkirchen, Germany.
[5]Also at Fraunhofer Institute for Atmospheric Environmental Research (IFU), Garmisch–Partenkirchen, Germany.

Paper number 98JD02676.
0148-0227/98/98JD-02676$09.00

total ozone. Reversing these considerations, *Pfeilsticker et al.* [1997] estimated the effect of pathlength enhancement on the absorption by atmospheric O_4 in relation to the cloud absorption anomaly [*Cess et al.*, 1995], which is a discrepancy between the observations and model calculations of the amount of solar radiation absorbed by clouds. All these findings, ranging from the cumulus effect to enhanced absorption of O_4 are manifestations of the same phenomenon: enhanced pathlength of radiation due to multiple scattering in clouds.

Here we investigate this phenomenon in the ultraviolet range of the solar spectrum, with special emphasis on (1) the consequences for the remote sensing of atmospheric parameters using measurements of scattered radiation at the Earth's surface and (2) the implications for our understanding of ultraviolet radiative transfer in clouds. Experimental observations under thunderstorm clouds give evidence for highly enhanced absorption in the presence of scattering media. This observation is quantitatively explained by calculation of photon pathlengths in clouds which can be enhanced by factors of 10 and more compared to cloudless sky. Under such circumstances, otherwise reliable methods for the determination of total ozone and cloud optical depth fail completely. Another important consequence is that possible changes in total ozone and cloudiness should not be considered separately in relation to their effect on the ground level UV irradiance.

2. Materials and Methods

2.1. Measurement System

All measurements were carried out on the roof platform of the Fraunhofer Institute for Atmospheric Environmental Research (IFU) in Garmisch–Partenkirchen, Germany (47.48°N, 11.07°E, and 730 m above sea level). The system for measuring spectral UV irradiance comprises a Bentham double monochromator DTM 300 with a photomultiplier as detector. Spectra of global irradiance are taken with a quartz cosine diffuser, and direct spectral irradiance is measured with narrow field-of-view entrance optics automatically aligned to the Sun. Both optics are coupled to the entrance slit of the monochromator with quartz fiber bundles. The deviations of the angular response of the diffuser from the ideal cosine law are corrected using an algorithm by *Seckmeyer and Bernhard* [1993]. To avoid errors arising from noise and variations in the photomultiplier dark current, an optical chopper is used in conjunction with a lock-in technique. The whole system is maintained at 20° ± 0.5°C. Calibrations are carried out in situ on a weekly basis using 100 W tungsten-halogen standard lamps. With a spectral resolution of 0.6 nm and a step width of 0.25 nm between 285 and 410 nm, approximately 100 spectra are taken every day with a typical scan duration of 10 min for this wavelength range. If the Sun is visible, spectra of direct and global irradiance are sampled alternately; otherwise, only global spectra are measured. The instrument has performed well in several intercomparisons of spectroradiometers [e.g., *Seckmeyer et al.*, 1994; *Gardiner and Kirsch*, 1995; *Seckmeyer et al.*, 1995]. Further instrumental details are given by *Seckmeyer et al.* [1996a]. The spectral measurements are supplemented with several ancillary sensors for quality control purposes and to provide complementary information. Of those, the data of an illuminance meter were used for the present study. This instrument measures broadband visible irradiance, i.e., illuminance, using a filter which resembles the sensitivity of the human eye, the so-called $V(\lambda)$ curve. The measurements of direct spectral UV irradiance are used to derive total ozone and spectral optical depth of the aerosol, τ_{Aerosol}, with a method described by *Mayer and Seckmeyer* [1996] and *Mayer et al.* [1997]. Aerosol extinction is parameterized with the Ångström turbidity formula $\tau_{\text{Aerosol}} = b\lambda^{-a}$, where λ is the wavelength in μm and a and b are Ångström's size exponent and turbidity coefficient, respectively.

2.2. Radiative Transfer Models

The optical properties of a plane-parallel atmosphere are fully described by three parameters: the extinction coefficient β, the single-scattering albedo ω, and the scattering phase function $p(\theta)$. All three parameters are functions of altitude. The radiative transfer models used in this study do not include the effects of polarization and Raman scattering. This is appropriate here because the uncertainties in the surface irradiance due to the neglect of polarization are generally smaller than 1–2% [*Lacis et al.*, 1998]. The effects of Raman scattering will be discussed in section 4.1. The extinction coefficient β is the sum of scattering coefficient β_{sca} and absorption coefficient β_{abs}. The single-scattering albedo $\omega = \beta_{\text{sca}}/(\beta_{\text{sca}} + \beta_{\text{abs}})$ describes the amount of scattering in the total extinction, and the phase function $p(\theta)$ is the probability distribution for scattering in any direction, where θ is the angle between the incident and the scattering directions. Related to the extinction coefficient β is the dimensionless optical depth τ which is defined as

$$\tau = \int_0^d \beta(z)\, dz \qquad (1)$$

where d is the total thickness of the medium. For a homogeneous medium with constant extinction coefficient β, (1) reduces to $\tau = \beta d$. Attenuation of a normal-incident parallel beam in a medium is described by Lambert–Beer's law:

$$E(d) = E(0)\exp(-\tau/\cos\theta) \qquad (2)$$

where E is the transmitted irradiance and θ is the angle between the direction of incidence and the surface normal.

Equation (2) only considers the attenuation of direct irradiance. Propagation of the scattered or dif-

fuse radiation is much more complicated and requires the solution of the equation of radiative transfer [*Chandrasekhar*, 1950]. Two different approaches were used in the present study: a one-dimensional model based on the discrete ordinate (DISORT) algorithm developed by *Stamnes et al.* [1988] and a specially developed Monte Carlo (MC) model which will be described below. To run the DISORT code, an interface is required to translate atmospheric parameters, like total ozone or aerosol and cloud properties, into input parameters for the model which are the extinction coefficient β, the scattering phase function $p(\theta)$, and the single-scattering albedo ω, all as functions of altitude. Here we used (1), a new implementation of the UVSPEC model described by *Mayer et al.* [1997], and (2), the tropospheric ultraviolet-visible (TUV) model by *Madronich* [1993]. It should be noted that these models are only different interfaces, used for convenience, for the same radiative transfer solver, DISORT.

The UVSPEC model was used to simulate the measured spectra while the TUV model was used to calculate the pathlength enhancement. The DISORT code within UVSPEC was run in six-streams mode and single precision, which is sufficient for simulation of measured spectra. In order to get accurate values for the sky radiance, the DISORT code within TUV was compiled in 64–streams mode and double precision. The latter was necessary because DISORT has a well-documented singularity for nonabsorbing atmospheres, that is single-scattering albedo $\omega \to 1$. If ω comes too close to 1, a small quantity, depending on the machine precision, is automatically subtracted from the single-scattering albedo, which can cause significant errors when the total optical depth is large.

The temperature-dependent ozone absorption cross section used for the calculations is from *Molina and Molina* [1986]; profiles of air pressure, temperature, and ozone concentration are midlatitude-summer profiles from *Anderson et al.* [1986]. The ground pressure was set to 930 mbar corresponding to the altitude of 730 m of the measurement site. The cloud optical properties were calculated using the parameterization developed by *Hu and Stamnes* [1993], which links microphysical parameters (effective droplet radius and liquid water content) of a cloud to its optical properties (extinction coefficient β, single-scattering albedo ω, and phase function $p(\theta)$). For the latter the Henyey–Greenstein phase function was used:

$$p(\theta) = \frac{1-g^2}{(1+g^2-2g\cos\theta)^{\frac{3}{2}}} \qquad (3)$$

Here g is the asymmetry factor, where $g = 0$ describes isotropic scattering, $0 < g < 1$ is biased in the forward direction, and $-1 < g < 0$ is biased in the backward direction. The Henyey–Greenstein phase function can be used instead of the more complicated phase functions calculated by Mie scattering theory. As has been shown by *Hansen* [1969], the Henyey–Greenstein phase function gives very accurate results for the irradiance transmitted and reflected by optically thick clouds. The value of the asymmetry factor for clouds in the UV range is approximately $g_{\text{cloud}} = 0.86$ [e.g., *Liou,* 1992; *Hu and Stamnes,* 1993].

While the DISORT model solves the radiative transfer equation for the radiance, the MC model traces a multitude of photons on their individual random paths. The MC model described here was especially designed for tracing photons in a homogeneous medium (see Figure 1 for details). As in the DISORT calculations, the Henyey–Greenstein phase function was used with an asymmetry factor of 0.86. For Monte Carlo calculations, the mean free pathlength s_{m} of a photon between two scattering events has to be known. The latter can be calculated using Lambert–Beer's law, (2), formulated for the number of transmitted photons, $N(s)$, which is proportional to the transmitted irradiance. $N(s) = N(0)\exp(-\beta_{\text{sca}}s)$ is the number of unscattered photons at the length s. The differential form of Lambert–Beer's law, $dN = N(s)\beta_{\text{sca}}ds$ gives the number of photons dN scattered between s and $s + ds$, and the mean free photon path finally evaluates to

$$s_{\text{m}} = \frac{\int_0^\infty s\,\exp(-\beta_{\text{sca}}s)\,ds}{\int_0^\infty \exp(-\beta_{\text{sca}}s)\,ds} = 1/\beta_{\text{sca}} \qquad (4)$$

In our MC model, photons travel in single, equidistant steps of one tenth of the mean free path. Thus the probability for a photon to be scattered after one step is simply 0.1. If a photon is scattered, a new random direction is chosen according to the phase function $p(\theta)$. Absorption is considered afterward, by weighting each traced photon with a Lambert–Beer factor of $\exp(-\beta l)$ where l is the pathlength traveled by the photon. This method has the advantage of (1) not reducing the number of photons during the tracing process, thereby improving the photon statistics, and (2) being computationally efficient by providing results for any amount of

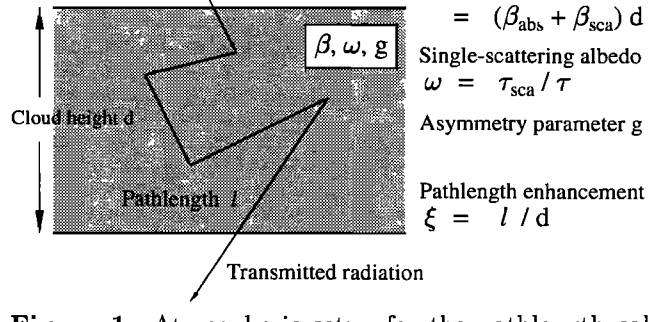

Figure 1. Atmospheric setup for the pathlength calculations: a single homogeneous cloud layer, described by its extinction coefficient β, single-scattering albedo ω, and the asymmetry parameter g of the Henyey–Greenstein phase function.

absorber within the cloud with one single Monte Carlo simulation. The transmittance of the medium, finally, is simply the number of photons leaving divided by the number of photons entering the medium. Each simulation for the present study was done by tracing 1,000,000 photons.

3. Experimental Observations

3.1. Spectral Measurements

On June 19, 1994, a thunderstorm cloud passed over Garmisch–Partenkirchen, Germany. Figure 2 shows the minute-by-minute measurements of the illuminance meter for this particular day. In the morning the sky was fairly clear with scattered clouds before noon. After noon, two cloud cases are clearly discernable, with the second one being a thunderstorm, where the illuminance dropped to only a few percent of its cloudless sky value. The effect of the thunderstorm on the spectral UV irradiance is shown in Figure 3. Although the Sun was approximately 24° degrees higher on the sky for the thunderstorm spectrum (case 2) than for the cloudless sky spectrum (case 1), the irradiance recorded during the thunderstorm is roughly 2 orders of magnitude smaller than the cloudless sky irradiance.

In order to quantitatively investigate the attenuation, the thunderstorm spectrum (case 2) was compared with a cloudless sky spectrum recorded at a comparable solar zenith angle (SZA) and comparable total ozone, see Figure 4 (thin line). Above 340 nm, where ozone does not absorb, the thunderstorm reduces the irradiance to roughly 2.5% of its clear sky value, showing very little dependence on the wavelength. For wavelengths where ozone absorption occurs, the reduction is stronger and increasing with decreasing wavelength. As the recording time of either spectrum is about 10 min, rapidly changing cloud conditions could create artificial wavelength dependent effects. However, this can be excluded for the presented cases, since the illuminance was stable within ± 5% ($\pm 1\sigma$) for the whole time of the scan, indicating that the strong spectral variation in the thunderstorm/clear ratio is not caused by changing cloud conditions.

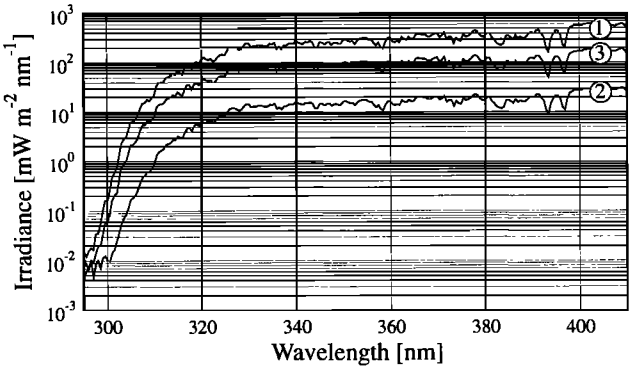

Figure 3. The measured UV spectral irradiance on June 19, 1994; case 1, 07:45 central European time (CET); case 2, 14:10 CET; and case 3, 16:30 CET. The solar zenith angles were 57°, 33°, and 54°, respectively.

3.2. Total Ozone and Cloud Optical Depth

The interpretation of measured spectra by model calculations requires knowledge of the atmospheric parameters, of which total ozone and cloud optical depth are the most important ones. Determination of to-

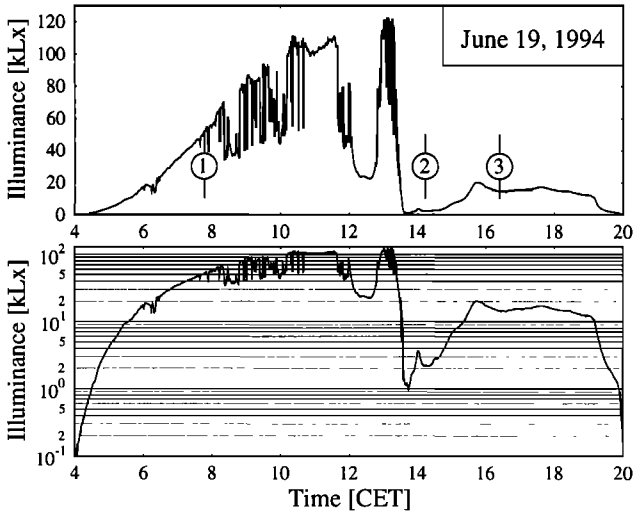

Figure 2. Diurnal variation of the illuminance on June 19, 1994, in Garmisch–Partenkirchen. The strong drop of the signal in the afternoon indicates the presence of very thick clouds. The markers indicate the recording times of the three spectra which are referred to as cases 1, 2, and 3 in the text.

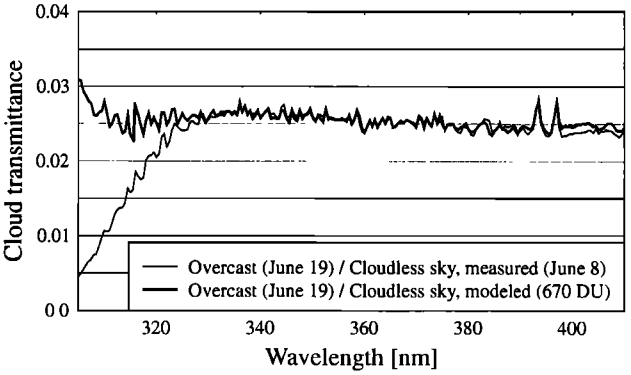

Figure 4. The ratio of the thunderstorm spectrum recorded at 14:10 CET, case 2, and a cloudless sky spectrum recorded on June 8, 10:30 CET (thin line). The solar zenith angle (57°) and total ozone (335 DU) for these two spectra are comparable. The ratio of the thunderstorm spectrum recorded at 14:10 CET and a cloudless sky model spectrum for a total ozone of 670 DU (thick line). Some of the structures, especially the two calcium lines between 390 and 400 nm which appear in both ratios are probably due to the so-called Ring effect (see text).

tal ozone under cloudy conditions is difficult because remote-sensing methods rely mostly on the attenuation of the direct solar beam. *Stamnes et al.* [1991] proposed a method for the simultaneous determination of total ozone and cloud optical depth from spectral global irradiance. The ozone determination is based on the evaluation of the ratio of the spectral global UV irradiance at two wavelengths, one with high ozone absorption (e.g., 305 nm) and one with low ozone absorption (e.g., 340 nm). A lookup table of the ratio as a function of solar zenith angle and total ozone is created using a radiative transfer model for a cloudless-sky atmosphere. By comparing measured ratios with those from the lookup table for a given solar zenith angle, the total ozone may be determined. For conditions where the Sun is visible, comparison with standard Dobson or Brewer measurements showed excellent agreement [*Mayer and Seckmeyer,* 1996; *Dahlback,* 1996]. The cloud optical depth is determined by comparing the irradiance at a wavelength where absorption by ozone is negligible with model-generated irradiances for various cloud optical depths. This independent determination of cloud optical depth and total ozone obviously relies on two assumptions: (1) The ratio of the irradiance at 305 and 340 nm is not influenced by the presence of clouds in first approximation, or, in other words, attenuation by clouds can be considered to be independent of wavelength and (2) scattering by clouds is the dominant effect in the UVA (315–400 nm), and other effects, like aerosol absorption, can be neglected. At a first glance, both assumptions seem to be reasonable because (1) the wavelength dependence observed, for example, by *Seckmeyer et al.* [1996b] is comparatively small compared to the wavelength dependence of ozone absorption and (2) the optical depth of the aerosol is usually negligible compared to the optical depth of a cloud. In the following it will be shown that neither assumption is valid for the observed case of a thick thunderstorm cloud.

Following the method of *Stamnes et al.* [1991], total ozone and cloud optical depth were calculated for all global spectra recorded on June 19, 1994 (see Figure 5). Total ozone and cloud optical depth calculated by this or similar algorithms are hereafter called "effective ozone" and "effective cloud optical depth" because they describe the combined effect of ozone absorption, aerosol scattering and absorption, and cloud scattering by means of equivalent or effective parameters which do not necessarily equal the actual ones. For our measurements we quite often observe a strong increase of the effective ozone in connection with optically thick clouds. In particular, for the described thunderstorm, case 2, an effective ozone of about 670 DU was obtained, whereas clear sky direct irradiance measurements before noon give a total ozone of 335 DU, in good agreement with the global irradiance ozone data (see Figure 5). A strong correlation between the effective ozone and the cloud optical depth is obvious.

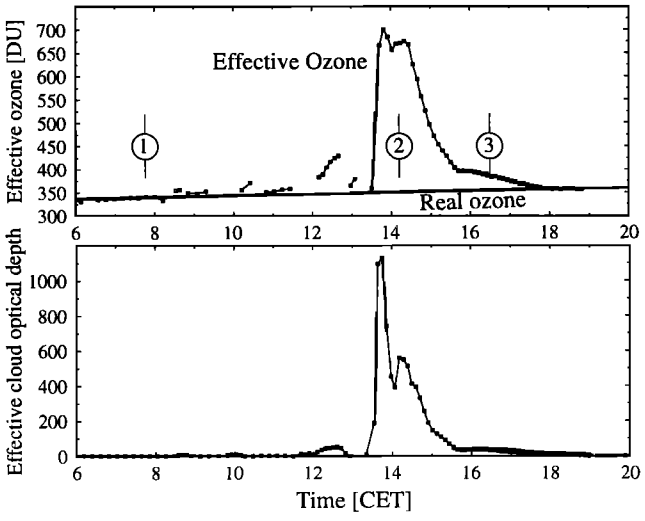

Figure 5. (top) Effective ozone, calculated from the wavelength pair 305 and 340 nm. Coincident with the large drop in the illuminance (Figure 2) is a sharp increase in the effective ozone. The real ozone is a linear interpolation between the values measured before and after the cloud occurred. (bottom) The effective cloud optical depth was calculated by comparing the measured irradiance at 380 nm with model generated irradiances for pure water clouds of variable optical depth [*Stamnes et al.*, 1991].

To nearly double the total ozone in less than an hour, up to an unreasonably high value of 670 DU, is not possible by any known chemical nor physical mechanism. In order to explain an extra column of 330 DU by ozone production in a thunderstorm cloud, the ozone mixing ratio had to be 800 ppb throughout the cloud, if the cloud height was assumed to be 8 km and if the mixing ratio was assumed to be constant with altitude. Such a high ozone production may be ruled out as, for example, *Ridley et al.* [1996] measured no increase but rather a small decrease in the ozone concentration within thunderstorm clouds in New Mexico. Hence the ozone determination method described by *Stamnes et al.* [1991] does not appear to be reliable under cloudy conditions. It should be noted that methods based on measurements of zenith radiance have similar problems [e.g., *Brewer and Kerr,* 1973; *Erle et al.,* 1995].

Figure 4 clearly illustrates the reason for the failure of the ozone determination method. Although it can be ruled out that the total ozone was actually 670 DU, we used the value as input to radiative transfer calculations in order to show that this unreasonable assumption could indeed explain the observations, if the cloud attenuation was assumed being spectrally flat. The thick line in Figure 4 shows the ratio between the thunderstorm spectrum and a calculated cloudless sky spectrum based on the effective ozone of 670 DU. Clearly, the strong wavelength dependence of the attenuation has vanished. Hence the thunderstorm observation might

be quite well modeled by a cloud attenuation which does not depend on wavelength and a total ozone of 670 DU under the assumption that multiple scattering within the cloud and ozone absorption can be treated independently. In the following sections we investigate the mechanism which makes the spectrum "look" like there were 670 DU of ozone.

4. Interpretation of the Measurements

4.1. Multiple Scattering

Scattering processes in a cloud lead to an enhancement of the photon path. If an absorbing constituent is present within the scattering medium, absorption will be enhanced compared to when the scattering medium is absent, due to the longer photon pathlength. This effect, although much smaller in magnitude than observed here, has been shown in several theoretical investigations. *Frederick and Lubin* [1988] as well as *Wang and Lenoble* [1996] calculated the transmittance of cloud layers of 0.5 km height. The described effects are clearly smaller than the one described here, because the amount of absorber inside a thunderstorm is much higher because of its larger vertical extent. A related phenomenon has been described by *Brühl and Crutzen* [1989], who investigated the effect of scattering by air molecules, droplets, and aerosol particles in the troposphere, leading to the "disproportionate role of tropospheric ozone as a filter against solar UVB radiation."

The following investigation focuses on the three cases shown in Figures 2 and 3. In the early morning of June 19, 1994, the sky over Garmisch–Partenkirchen was cloud free. Ozone and aerosol information from direct spectra obtained during this period were used for the simulations of the overcast situations later in the day. The total ozone was taken to be 335 DU for case 1 and increased to 345 DU for cases 2 and 3 in accordance with the change of the total ozone inferred from measurements before and after the clouds occurred. The aerosol optical depth was parameterized by the Ångström formula with coefficients measured in the morning, $a = 1.147$ and $b = 0.20$, corresponding to an optical depth of 0.69 at 340 nm.

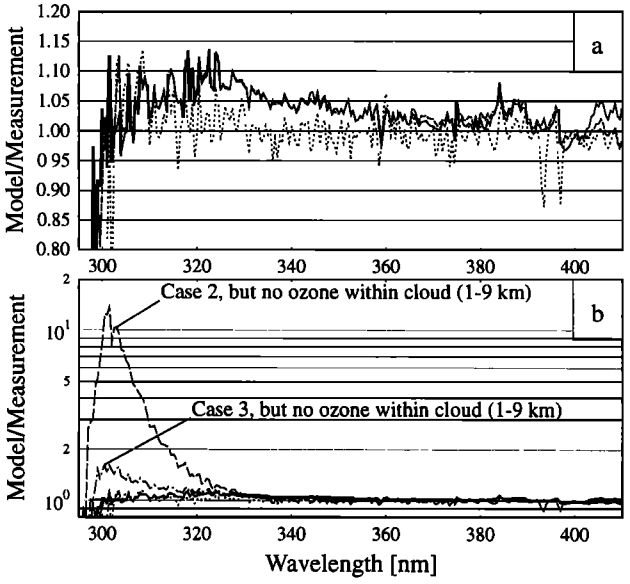

Figure 6. (a) The ratio of model and measurement for the three cases in Table 1, case 1 (solid line), case 2 (dotted line), and case 3 (dashed line). (b) Same as (a), but the thunderstorm (case 2) and the afternoon cloud (case 3) without ozone inside the clouds have been included. Case 2 clearly demonstrates that the small fraction of ozone within the cloud (less than 10% of the total column) causes reduction by more than a factor of 10 of the global irradiance at short UV wavelengths.

The clear sky case is well reproduced by the model (see Figure 6a). The deviations are similar to those discussed by *Mayer et al.* [1997]. For the overcast cases, a homogeneous cloud was introduced. A reasonable value was adopted for the effective droplet radius (10.5 μm). The difference between measured and modeled spectra was then minimized by variation of the optical depth and the vertical position of the cloud. The resulting atmospheric parameters which are shown in Table 1 allowed the simulation of all measured spectra to within $\pm 10\%$ (see Figure 6a). It should be noted that the cloud had certainly a more complicated structure and that the chosen parameters are somewhat arbitrary. Nevertheless, it can be concluded that the measured spectrum

Table 1. Model Input Parameters

Case	Time, UT	Solar Zenith Angle	Cloud Extent, km	Effective Droplet Radius, μm	Cloud Optical Depth	Real Total Ozone, DU
1	0746	57	–	–	–	335
2	1410	33	1.0–9.0	10.5	340	345
3	1630	54	1.0–9.0	10.5	32	345

The cloud optical properties were calculated from the estimated cloud height, effective droplet radius, and the liquid water content, using the parameterization of *Hu and Stamnes* [1993]. The cloud optical depth was adjusted to give the best agreement between model and measurements. For all simulations, the aerosol optical depth was calculated from the Ångström formula with $a = 1.147$ and $b = 0.20$. The aerosol single-scattering albedo was set to 0.95, and the asymmetry factor was 0.7.

can be quantitatively described using a reasonable guess of the atmospheric conditions based on the available observations.

In order to demonstrate the interaction between cloud scattering and ozone absorption, the ozone concentration was first set to zero within the vertical extension of the model cloud (1–9 km) and the resulting ozone profile was rescaled to 345 DU (see Figure 6b). The effect on the cloud-covered cases, 2 and 3, is striking: Redistribution of the ozone results in an increase in the irradiance of more than a factor of 10 at 300 nm for the thunderstorm cloud (case 2). Even for the optically much thinner afternoon cloud (case 3) a remarkable increase can be observed. This clearly indicates that absorption by ozone is strongly enhanced in the presence of multiple scattering.

It has already been noted that the above set of input data is definitely not the only one that can be used to model the observed thunderstorm spectrum. As an example, we varied the aerosol optical depth and readjusted the other parameters to optimize the agreement between model and measurement. Reducing the aerosol optical depth to 0 has a striking effect on the model atmosphere: In order to reach agreement again, the cloud optical depth had to be increased from 340 to 560, and the ozone amount in the cloud had to be reduced from 26.9 to 15.7 DU by lowering the cloud top from 9 to 6 km. Missing information about the aerosol therefore introduces high uncertainty into the derived scattering optical depth of the cloud. The effect of the aerosol is surprisingly high considering that the measured extinction optical depth of the aerosol of 0.69 at 340 nm is negligible compared to the optical depth of the cloud. Aerosol particles, however, are more efficient absorbers in the UV range than pure water droplets, their single-scattering albedo being usually in the range of 0.8–1.0, compared to that of water droplets of 0.999990–0.999999 [*Hu and Stamnes*, 1993]. The absorption optical depth of the aerosol is therefore at least 10 times larger than the absorption optical depth of the cloud. Furthermore, aerosol absorption is enhanced owing to multiple scattering. In summary, it can be concluded that the transfer of radiation through the observed cloud is influenced mainly be three parameters: the optical depth of the cloud, the amount of ozone within the cloud, determined by the ozone profile and the vertical position of the cloud, and the absorption optical depth of the aerosol. These three parameters are coupled nonlinearely in their effect on UV irradiance.

A different effect which is also very likely to be caused by multiple scattering inside the cloud is obvious in Figures 4 and 6. In the region of strong Fraunhofer lines a relative enhancement of the irradiance, compared to adjacent wavelengths, can be observed for spectra measured under thick clouds. This is most obvious at the two calcium lines between 390 and 400 nm. Such behavior was first observed by *Grainger and Ring* [1962] and is consequently called the "Ring effect." It is caused by rotational Raman scattering by air molecules and tends to fill in the Fraunhofer lines [*Joiner et al.*, 1995]. A pathlength enhancement due to cloud scattering directly affects the average number of times a photon is Rayleigh scattered, and by the same amount the average number of times a photon is Raman scattered. The Ring effect is therefore much enhanced by the presence of the cloud and becomes clearly visible in the ratios in Figures 4 and 6.

4.2. Pathlength Enhancement in a Homogeneous Medium

The investigation in section 4.1 showed that the photon path is increased owing to the presence of a scattering medium, leading to a larger effective absorption optical depth, which is the product of the absorption coefficient and the pathlength through the absorbing medium. An increased absorption optical depth can therefore be interpreted either correctly by means of an enhanced pathlength, or wrongly as an increased total ozone, as it happens when the method of *Stamnes et al.* [1991] is applied during thick clouds without care. In order to explain a doubling in the effective ozone, however, large pathlength enhancements are required, considering that only a small fraction of the total ozone is inside the cloud.

Pathlength enhancements can be calculated using a Monte Carlo model which traces single photons on their way through the atmosphere [e.g., *Feigelson,* 1984; *Dianov-Klokov and Krasnokutskaja,* 1972; *Kargin et al.,* 1972]. The MC model was used to calculate the pathlength probability distribution $p_0(\vec{x}, l)$ for a purely scattering medium without absorption, where $p_0(\vec{x}, l)dl$ is the probability that a transmitted photon which arrives at a point $\vec{x}$ traveled a pathlength between l and $l + dl$ [see, e.g., *Feigelson,* 1984]. With knowledge of $p_0(\vec{x}, l)$, the average pathlength l_{avg} for transmitted photons is evaluated immediately:

$$l_{\text{avg}}(\vec{x}) = \int_0^\infty p_0(\vec{x}, l) l \, dl \tag{5}$$

Here $p_0(\vec{x}, l)$ is obviously dependent on the optical properties of the layer but also on the radiance distribution entering the medium. In the plane-parallel case the pathlength probability distribution of the photons leaving the cloud base does not depend on the location $\vec{x}$ and $p_0(\vec{x}, l)$ reduces to $p_0(l)$.

For the special case of a homogeneously distributed absorber, knowledge of the pathlength probability distribution $p_0(l)$ for the nonabsorbing medium is sufficient to calculate the transmitted irradiance E for any amount of absorber:

$$E = E_0 \cdot \int_0^\infty p_0(l) \exp(-\beta_{\text{abs}} l) \, dl \tag{6}$$

where E_0 is the transmitted irradiance for the nonab-

sorbing medium. Equation (6) is simply the application of Lambert–Beer's law for each photon traversing the cloud. It should be noted here that the Monte Carlo method is not the only one for calculating pathlength probability distributions. *Bakan and Quenzel* [1976], for example, employed inverse Laplace transformation for aerosol-loaded atmospheres, and *van de Hulst* [1980] compiled investigations of various authors in order to approximate average photon pathlengths analytically. The Monte Carlo method, however, is the most straightforward approach, avoiding uncertainties introduced by simplifying assumptions which are required by the other methods.

A completely different approach to calculate pathlength enhancements is a macroscopic definition of an "effective pathlength" l_{eff} by comparing the irradiance E in presence of the absorber with the irradiance E_0 without the absorber [e.g., *Feigelson,* 1984; *Kurosu et al.,* 1997]:

$$E = E_0 \exp(-\beta_{\text{abs}} l_{\text{eff}}) = E_0 \exp(-\tau_{\text{abs}} \xi_{\text{eff}}) \quad (7)$$

where $\xi_{\text{eff}} = l_{\text{eff}}/d$ is the "effective pathlength enhancement" and d is the geometrical height of the layer. Equation (7) is a parameterization of global irradiance by a Lambert–Beer type law. Note that this definition refers to the vertical optical depth of the cloud. In consequence, a ray passing the medium under an incidence angle θ is subject to a pathlength enhancement of $(1/\cos\theta)$ due to pure geometrical reasons even without scattering.

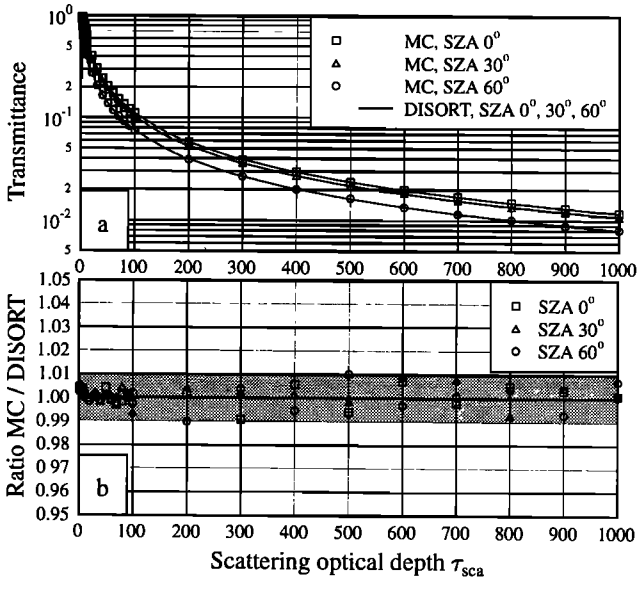

Figure 7. Model results for a homogeneous, nonabsorbing layer. (a) Cloud transmittance as a function of the optical depth, calculated by the DISORT and MC models for three solar zenith angles. (b) Ratio of the transmittance calculated by the MC and the DISORT models; the agreement between both models is better than ±1%.

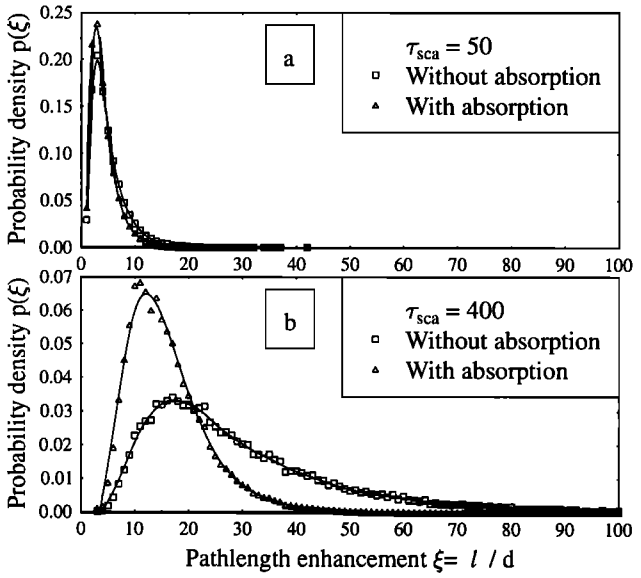

Figure 8. Pathlength probability distribution p(ξ) for transmitted photons, calculated by the MC model and sampled in bins of 1 km. (a) Cloud optical depth 50 and (b) cloud optical depth 400 are shown. All probability distributions are normalized to a total probability of 1. The effect of an absorber of optical depth 0.1 in the cloud can be clearly seen. The solid curve is a spline approximation of the data points.

The effective pathlength l_{eff} is easily available from (7) by computing E and E_0 using an arbitrary radiative transfer model. If all photons traveled the same length and consequently obeyed Lambert–Beer's law, l_{eff} would obviously be equivalent to the real or average photon pathlength, l_{avg}. In the case of very small absorption, $\beta_{\text{abs}} l \ll 1$, the exponential function in (6) can be replaced by its linear approximation:

$$\begin{aligned} E &= E_0 \int_0^\infty p_0(l)(1 - \beta_{\text{abs}} l) dl \\ &= E_0(1 - \beta_{\text{abs}} l_{\text{avg}}) \end{aligned} \quad (8)$$

Comparing this with (7), it can be concluded that effective and average pathlengths equal in the limit of small absorption. This is not self-evident because the definitions of both parameters are completely different. While the effective pathlength is a parameterization of the observed effects, the average pathlength gives a closer view of the physics, being based on the microscopic photon path.

In the following we present the results of transmittance and pathlength calculations using the DISORT and the MC models. Figure 7 shows the transmittance of a nonabsorbing layer as a function of its scattering optical depth, calculated for three incidence angles: The results of both models agree within ±1% for optical depths between 1 and 1000 (Figure 7b). This agreement is remarkable, considering the completely different approaches. The small difference is within the sta-

tistical uncertainty of the MC model, which is about $\pm 0.6\%(\pm 2\sigma)$ at optical depth 100 and $\pm 2\%$ at optical depth 1000, where the transmittance drops to about 10% and 1%, respectively. The transmittance of the layer decreases with increasing incidence angle.

Figure 8 shows an example of the pathlength probability distribution $p(\xi)$, calculated by the MC model. In the case of absorption, $p(\xi)$ is the product of $p_0(\xi)$ and the Lambert–Beer factor $\exp(-\tau_{\text{abs}}\xi)$, renormalized to a total probability of 1. The distribution is shifted toward higher pathlength enhancement when the scattering optical depth increases from $\tau_{\text{sca}} = 50$ (Figure 8a) to $\tau_{\text{sca}} = 400$ (Figure 8b). Also clearly visible is a shift toward smaller pathlengths when an absorber of optical depth $\tau_{\text{abs}} = 0.1$ is added to the cloud. At 305 nm, this amount of absorption corresponds to 21 DU of ozone. This number is roughly the amount of ozone in a thick tropospheric cloud based on the midlatitude-summer profiles from *Anderson et al.* [1986], which were used throughout this study.

Figure 9 shows the effective and average pathlength enhancements, ξ_{eff} and ξ_{avg}, calculated with the MC and DISORT models according to (5) and (7), respectively. The filled markers and the solid line refer to a nonabsorbing cloud, i.e., no absorption in the MC model, and a very small test absorber in the DISORT model, described by a single-scattering albedo of $\omega = 0.999999$. As was derived analytically above, average and effective pathlength enhancements agree very well for nonabsorbing clouds. The systematic deviation of up to 5% for high optical depths is due to numerical problems arising in the comparison of nearly identical values of E and E_0 in (7). These uncertainties are probably due to the mentioned DISORT instability for single-scattering albedos close to 1, even with the double-precision version of DISORT. As the magnitude of the error cannot be easily estimated, the MC simulation is essential to check the validity of the DISORT results for thick, nonabsorbing clouds. Figure 9b shows a zoom of Figure 9a for low optical depths. Here a distinct dependence on solar zenith angle is obvious, which is easily explained by the definition of the pathlength enhancement: For thin clouds, a significant fraction of the transmitted photons leaves the cloud base unscattered with a pathlength enhancement of $1/\cos\theta$ (see the explanation of (7)). In the limit of small scattering optical depth, $\tau_{\text{sca}} \to 0$, the three curves approach $1/\cos 0° = 1.0$, $1/\cos 30° = 1.155$, and $1/\cos 60° = 2.0$. The zenith angle dependence vanishes with increasing optical depth of the cloud. These results are in quantitative agreement with the findings of *Plass and Kattawar* [1968] and *Kurosu et al.* [1997].

An angularly resolved MC calculation of the average pathlength enhancement $l_{\text{avg}}(\vec{r})$ showed that for $\tau_{\text{sca}} > 25$ the variation of $l_{\text{avg}}(\vec{r})$ with the direction $\vec{r}$ is less than $\pm 5\%$, while for $\tau_{\text{sca}} > 70$ it is even less than $\pm 1\%$. Hence, for optically thick clouds $l_{\text{avg}}(\vec{r})$ exhibits very little dependence on the direction $\vec{r}$ of the photon leaving the cloud base. In consequence, all findings for the irradiance are also valid for the radiance.

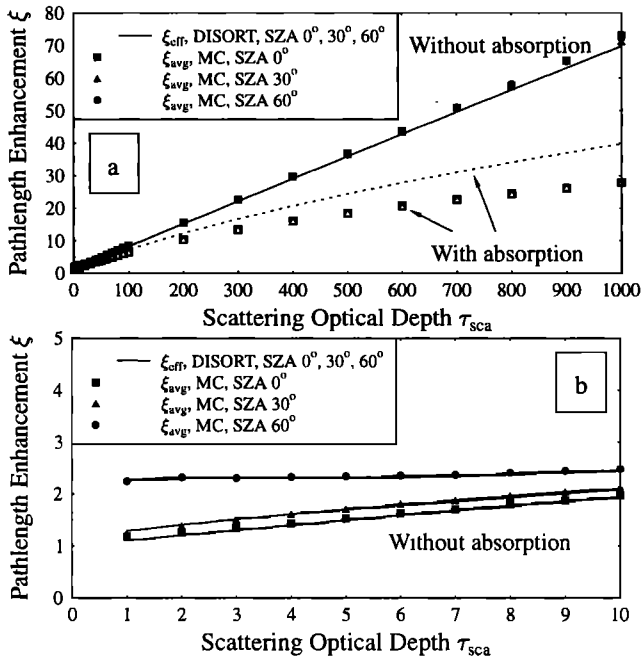

Figure 9. Model results for a homogeneous, nonabsorbing cloud layer. (a) Effective and average pathlength enhancement, calculated by the DISORT and MC models, respectively. (b) Zoom of the small optical depth part of (a). For low optical depths a zenith angle dependence of the pathlength enhancement is obvious, while for high optical depths there is no visible dependence.

Consideration of an absorber is somewhat different in our case compared to previous studies which focussed mostly on the visible and infrared bands of the spectrum, where absorption usually cannot be treated monochromatically, because such so-called line-by-line calculations are very time consuming. Instead, absorption bands in the visible and infrared are parameterized by functions deviating from Lambert–Beer's law, preventing a direct comparison of these results with our data [e.g., *Dianov-Klokov and Krasnokutskaya,* 1972]. The open symbols and dashed lines in Figure 9a show the results for an absorbing layer of optical depth $\tau_{\text{abs}} = 0.1$. At 305 nm, this amount of absorption corresponds to 21 DU of ozone, which is a reasonable guess for the ozone amount in a tropospheric cloud. As expected, both effective (DISORT) and average (MC) pathlength enhancements decrease with increasing absorption because the long paths are more suppressed by the exponential Lambert–Beer attenuation factor than the short ones (see (6)). In addition, average and effective pathlengths differ remarkably, due to the fact that the assumption of small absorption, $\beta_{\text{abs}} l \ll 1$, which was necessary to derive (8), no longer holds in this case. Note that this is not due to a numeric problem but to the conceptual difference between effective and average

pathlengths. While the effective pathlength describes the effect on the transmitted irradiance, the average pathlength resembles the actual path of the photons through the atmosphere. They are equal only in the limit of small absorption.

Figure 9 shows that photons leaving the base of thick clouds indeed traveled over tenfold– to hundredfold a distance compared to the geometrical cloud height d. The special case of the nonabsorbing medium (solid line and filled symbols) deserves special attention: The average pathlength enhancement ξ_{avg} is in very good approximation directly proportional to the scattering optical depth τ_{sca}. Considering that the mean free path of a photon between two scattering events is $1/\beta_{\text{sca}}$, the average number of scattering events N_{avg} for a photon is

$$N_{\text{avg}} = l_{\text{avg}}\beta_{\text{sca}} = \xi_{\text{avg}}\tau_{\text{sca}}. \quad (9)$$

Introducing the proportionality between ξ_{avg} and τ_{sca}, which is obvious from Figure 9, one finds that $N_{\text{avg}} \propto \tau_{\text{sca}}^2$, or

$$d \propto \sqrt{N_{\text{avg}}}\frac{1}{\beta_{\text{sca}}}. \quad (10)$$

This formula resembles the solution of the "random walk" problem when the cloud height d is interpreted as the root mean square distance of a photon from its starting point after N_{avg} scattering events with a mean free path of $1/\beta_{\text{sca}}$ [e.g., *Parzen,* 1960].

4.3. Pathlength Enhancement for a Real Atmosphere

The results presented in section 4.2 for a single layer with homogeneous optical properties, though being very helpful for the understanding of the underlying processes, are somewhat academic, as the simplified setup does by no means resemble a real atmosphere. Furthermore, the large pathlength enhancements calculated in section 4.2 are effective only within the cloud, and the net effect therefore depends on the fraction of the absorber inside the cloud which in the case of ozone is usually less than 10%. In order to account for these effects, the above DISORT calculations were repeated for six different atmospheric setups, where a homogeneous cloud was placed between 1 and 9 km, and step-by-step other atmospheric components were added; in particular these were a Rayleigh atmosphere, an ozone profile, an aerosol profile, and a nonzero surface albedo. Unlike the calculations in section 4.2, the test absorber, necessary for the calculation of the pathlength enhancement according to (7), was now not confined to the cloud but distributed over the whole atmosphere by means of a realistic ozone profile instead of adding a constant amount of absorption. In consequence, the calculated pathlength enhancement no longer describes the pathlength enhancement of radiation within the cloud but rather the increase of the optical depth considering the whole atmosphere, which is the relevant parameter when looking at unusually high total ozone derived from global irradiance measurements. In order to avoid confusion, we therefore replace the term "pathlength enhancement" by "optical depth enhancement" in this context, although the mathematical formulation of both is identical.

The following six atmospheres were investigated: A, homogeneous cloud between 1 and 9 km without surrounding atmosphere, as in section 4.2; B as A, but with additional Rayleigh atmosphere; C as B, but with total ozone of 320 DU; D as C, but with an additional aerosol profile according to *Elterman* [1968], with a total optical depth of 0.38 at 340 nm and a single-scattering albedo of 0.95; E as D, but with surface albedo of 0.1 (snow free); and F as E, but with surface albedo of 0.8 (snow covered). Profiles of air pressure, temperature, and ozone concentration are midlatitude-summer profiles from *Anderson et al.* [1986]; the ground pressure is 930 mbar corresponding to the altitude of 730 m at the measurement site. The choice of the ozone profile for these calculations is much more important than for cloudless sky model calculations because the profile together with the cloud top and bottom determines the amount of absorber in the cloud. For cases A and B the ozone profile scaled to a total column of 1 DU was used as test absorber for (7), while for atmospheres C–F the entire column of 320 DU was employed as test absorber.

Figure 10 shows the results of these calculations for a solar zenith angle of 30°. Figure 10a presents the transmittance at 340 nm, which is related to the optical depth of the cloud, and the optical depth enhancement at 305 nm, which determines the effective ozone calculated by the method of *Stamnes et al.* [1991]. Figure 10a indicates that the transmittance at 340 nm is mostly determined by the cloud rather than by the surrounding atmosphere: Atmospheres A–C give very similar results. Rayleigh scattering therefore does not introduce large corrections, as it can be expected when considering the comparatively small Rayleigh scattering optical depth of only 0.65 at 340 nm. The effect of ozone absorption on the transmittance at 340 nm is also very small, due to the negligible absorption cross section of ozone at 340 nm. Absorption by aerosol, however, introduces a considerable decrease in the transmittance, see the plot for atmosphere D. In contrast, a nonabsorbing aerosol would not change the transmittance significantly, as has been verified by recalculation of D with a single-scattering albedo of 1. The large decrease is therefore due to the small amount of aerosol absorption, as was already indicated in section 4.1. Ground albedo causes also large changes, especially for optically thick clouds. Introducing a surface albedo of 0.8, which is a reasonable value for completely snow covered ground, increases the irradiance under the cloud by a factor of 4. The underlying mechanism is the trapping of radiation between surface and cloud bottom.

Figure 10b shows the optical depth enhancement ξ_{eff} at 305 nm, calculated for the six atmospheres. Atmo-

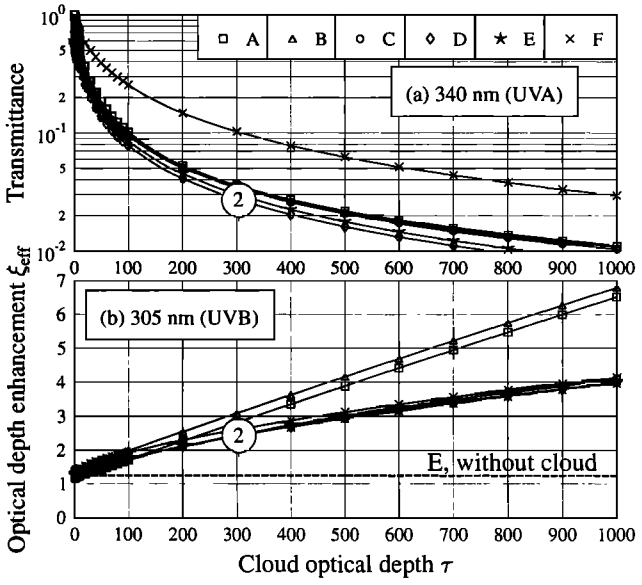

Figure 10. Calculations for various atmospheres: A isolated homogeneous cloud; B as A, but with additional Rayleigh atmosphere; C as B, but with total ozone of 320 DU; D as C, but with additional aerosol according to *Elterman* [1968]; E as D, but with a surface albedo of 0.1 (snow free); and F as E, but with a surface albedo of 0.8 (snow covered). (a) Transmittance of the cloud at 340 nm (UVA) and (b) optical depth enhancement at 305 nm (UVB) are shown. The label 2 indicates the conditions of case 2 which has been investigated before, characterized by atmospheric setup E and a UVA transmittance of 0.027. The dashed curve shows the optical depth enhancement for atmosphere E without clouds, $\xi_{\text{eff,Rayleigh}}$; the latter conditions are the basis for the total ozone determination method proposed by *Stamnes et al.* [1991].

sphere A reproduces the result of the single-layer calculations of section 4.2 considering that here only a small fraction of the test absorber is inside of the cloud while the major part of the ozone is not subject to pathlength enhancement. In this example with the cloud lying between 1 and 9 km, only 8% of the total ozone is within the cloud. Introducing a total ozone of 320 DU to the total ozone (curve C) has the most pronounced effect on the pathlength enhancement, reducing it by about one third for high cloud optical depths. The effects of Rayleigh scattering, aerosol scattering and absorption, and ground albedo on the pathlength enhancement are comparatively small.

When calculating the effect of the optical depth enhancement in a cloudy atmosphere, it has to be considered that the optical depth enhancement in a cloudless atmosphere is also larger than 1, due to the slant path of the radiation and the Rayleigh scattering. The dashed line in Figure 10b shows the optical depth enhancement for atmosphere E without a cloud, $\xi_{\text{eff,Rayleigh}}$. Calculations with the DISORT model for a pure Rayleigh atmosphere show that the optical depth enhancement of the cloudless atmosphere $\xi_{\text{eff,Rayleigh}}$ can be approximated by $1/\cos\theta$ within 10% accuracy for all solar zenith angles between 0° and 60° and total ozone between 0 and 1000 DU, indicating that the effective photon path in a Rayleigh atmosphere is very close to the path of directly transmitted radiation.

The combination of Figures 10a and 10b allows the estimation of the pathlength enhancement for the measurement of June 19, 1994, case 2. From Figure 4 the transmittance at 340 nm is found to be 0.027, which corresponds to an optical depth of 304 according to Figure 10a, atmosphere E. From Figure 10b it follows that the corresponding optical depth enhancement is 2.43, compared to a cloudless sky optical depth enhancement of 1.24. Applying the ozone determination method described by *Stamnes et al.* [1991] for the heavily overcast case 2 results in an overestimation of the optical depth by a factor of 2.43 / 1.24 = 1.96. In consequence, the total ozone, which is directly proportional to the optical depth, will be overestimated by a factor of 1.96 which is very close to the experimentally determined factor of 670 DU / 335 DU = 2.0 (see Figure 5). Because of the slightly different model setup for these calculations, the numbers may differ from those section 4.1.

4.4. UVA Transmittance and Effective Ozone

In order to prove that the thunderstorm on June 19, 1994, was not an isolated incident, the period from 1994 to 1996 was searched for episodes where (1) the effective ozone exceeded 600 DU for at least five consecutive data points and (2) the Sun was visible before and after the

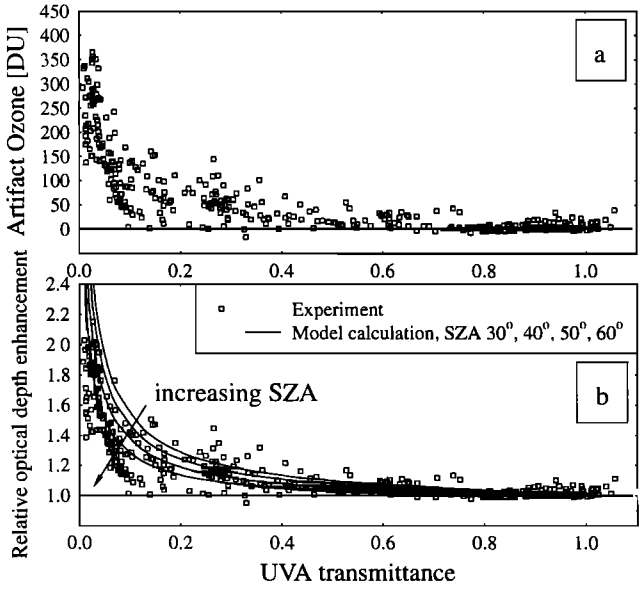

Figure 11. (a) Experimentally determined artificial ozone (difference between effective and real ozone) as a function of UVA transmittance. (b) Relative optical depth enhancement, $\xi_{\text{eff}}/\xi_{\text{eff,Rayleigh}}$, determined experimentally (squares) and by model calculation (line). The correlation between both data sets is obvious.

cloud occurred, enabling the determination of the real total ozone. Assuming that the total ozone had not changed considerably between the observations before and after the occurrence of the cloud, the difference between the effective ozone and the real total ozone was calculated, which in the following is referred to as "artifact ozone." This parameter is shown in Figure 11a as a function of the UVA transmittance. The latter was calculated as the ratio between measured and modeled cloudless sky UVA irradiance. The plot clearly indicates a systematic overestimation of the total ozone of up to several 100 DU if the cloud transmittance is smaller than 10%. But even for thinner clouds, considerable deviations of up to 100 DU may occur.

In order to compare these findings with the model results shown in section 4.3, the optical depth enhancement ξ_{eff} was calculated for each measured data point. As explained above, the ratio of the effective and the real total ozone is equivalent to the relative optical pathlength enhancement $\xi_{\text{eff}}/\xi_{\text{eff,Rayleigh}}$, which is plotted in Figure 11b. Also plotted is the same ratio, calculated by the DISORT model for atmosphere E for four solar zenith angles. Both data sets are generally in good agreement, although the measured data points tend to be somewhat lower than the modeled data points. This discrepancy could of course be avoided by tuning the ozone and aerosol profiles as well as the cloud bottom and top heights. However, as these data are not available for the chosen situations, we do not follow this point any further.

5. Summary and Conclusions

Our observations and interpretations of the radiative transfer in optically thick clouds have demonstrated that atmospheric absorption can be significantly enhanced owing to the presence of a scattering medium. There are various consequences for the interpretation of ultraviolet irradiance at the Earth's surface.

1. Enhanced absorption is most pronounced in the case of ozone, the dominant absorber in the UVB range. The relative increase, however, was much higher for the aerosol absorption because a much larger fraction of the total atmospheric aerosol is inside the cloud and therefore subject to the enhancement. As the underlying mechanism is of course not restricted to ozone and aerosol, it can be concluded that signatures of other species, especially those predominantly available in the troposphere (like sulfur dioxide or nitrogen dioxide) are also enhanced in presence of clouds and might become noticeable in global irradiance spectra.

2. The observed coupling between scattering and absorption prevents the independent determination of atmospheric parameters from spectral irradiance measurements under thick clouds, although this is possible for cloudless sky and probably thin clouds in good approximation [*Stamnes et al.*, 1991]. For the interpretation of our measurements the following two couplings are of the highest importance: (1) Neglecting the coupling between cloud scattering and ozone absorption leads to an overestimation of the derived total ozone, in our example by 300 DU which is a factor of 2 and (2) neglecting the coupling between cloud scattering and aerosol absorption leads to an overestimation of the actual cloud optical depth. These mechanisms prevent the use of simple lookup tables and require full radiative transfer calculations considering all relevant parameters instead.

3. Total ozone, determined from global sky irradiance according to *Stamnes et al.* [1991], has been shown to agree within 1–2% with standard Dobson or Brewer measurements when the direct Sun was visible [*Mayer and Seckmeyer,* 1996; *Dahlback,* 1996]. During heavily cloud covered sky, however, the errors found in this study are much higher than those estimated by *Stamnes et al.,* [1990, 1991] and *Høiskar et al.* [1997], who all calculated the error to be less than 10% for cloud optical depths up to 100. The marked difference between those estimates and our findings is due to two facts: (1) The amount of ozone within the cloud was much smaller for all the cited papers, due to the smaller vertical extent of the cloud of less than 2 km and (2) the optical depth of the observed thunderstorm cloud was much higher than those investigated by the other authors. Our experimental study shows that the total ozone may be easily overestimated by a factor of 2 and more if the cloud transmittance is below 5% and even for a transmittance as high as 30–40%, errors of up to 50 DU may occur. Chosing a pair of closer wavelengths would not reduce the error, because all wavelengths are subject to the pathlength enhancement. It should also be noted that the error decreases with increasing solar zenith angle and decreasing tropospheric ozone amounts.

4. The finding that the pathlength enhancement does not depend on the angle under which radiation leaves the base of a thick cloud allows the conclusion that all methods which derive trace gas abundances from scattered transmitted radiation are subject to the same amount of error. Consequently, there is little extra information to be gained from radiance measurements. This has already been demonstrated by *Erle et al.* [1995] for the ozone determination from zenith sky radiance. Satellite remote-sensing methods, employing the back-scattered radiation, are much less sensitive to this type of error because the pathlength enhancement of reflected radiation is typically only about 2 [*Kurosu et al.*, 1997].

5. The best way to avoid errors in the derived total ozone due to the presence of clouds is to discard the data when the measured UVA irradiance is below a certain lower limit, a strategy followed for example by *Fioletov et al.* [1997]. Correction of the error would require knowledge of the profiles of the ozone concentration and the aerosol absorption coefficient throughout the cloud; both are not easily available. Alternatively, a closer investigation of the spectral dependence of the cloud

transmittance shows that the latter contains information about the amount of ozone in the cloud because the pathlength enhancement decreases with increasing absorption optical depth and consequently with decreasing wavelength. This results in a dependence of the effective ozone on the lower wavelength used for the derivation which could be used to infer the amount of absorber inside the cloud. More sensitivity studies would be required in order to investigate this possibility, considering the limitations of a real measurement system. The bold line in Figure 4 shows in fact a slight increase of the ratio of measured spectrum and the model calculation based on the effective ozone, indicating a decrease in the effective ozone toward smaller wavelengths.

6. The finding that total ozone derived from scattered radiation is unreliable under thick clouds is of important consequence for experimental studies of the effect of clouds on surface irradiance. Considering the effective ozone as real would lead to completely wrong conclusions about the wavelength dependence of cloud attenuation.

7. The coupling between scattering and absorption is important for the estimation of surface UV irradiation because it introduces strong wavelength dependence into cloud attenuation, which tends to reduce UVB irradiance much more than UVA. In consequence, changes in total ozone and changes in cloudiness are coupled nonlinearly in their influence on surface UV irradiance. Although enhanced absorption does only occur in presence of thick clouds when the irradiance is low anyway, it could have an influence on trends of ultraviolet irradiance which are expected to be comparatively small numbers.

The UVSPEC radiative transfer model used to simulate the measured spectra and to retrieve the total ozone and cloud optical depth is part of the libRadtran package which is available by anonymous ftp to ftp.geofysikk.uio.no, cd pub/outgoing/arveky. The TUV V3.9 radiative transfer model used for the pathlength enhancement calculations is available by anonymous ftp to acd.ucar.edu, cd /user/sasha.

Acknowledgments. This study has been funded by the German ministry of Education, Science, Research and Technology (BMBF) and the European funded SUVDAMA project (contract ENV4-CT95-0177). B.M. was supported by a research grant by the German Academic Exchange Service (DAAD). A.K. acknowledges support by the Norwegian Research Council. S.M. was supported by the Department of Energy through grant No. DE-A 105-94ER61879 to NCAR. NCAR is sponsored by the National Science Foundation. Finally we wish to thank Edeltraud Leibrock, Germar Bernhard, and Astrid Albold for their valuable comments and suggestions.

References

Anderson, G., S. Clough, F. Kneizys, J. Chetwynd, and E. Shettle, AFGL Atmospheric Constituent Profiles (0-120 km), AFGL-TR-86-0110, Air Force Geophys. Lab., Hanscom AFB, Mass., 1986.

Bakan, S., and H. Quenzel, Path length distributions of photons scattered in turbid atmospheres, *Beitr. Phys. Atmos.*, *49*, 272–284, 1976.

Brewer, A. W., and J. B. Kerr, Total ozone measurements in cloudy weather, *Pure Appl. Geophys.*, *106–108*, 929–937, 1973.

Brühl, C., and P. J. Crutzen, On the disproportionate role of tropospheric ozone as a filter against solar UV-B radiation, *Geophys. Res. Lett.*, *16*, 703–706, 1989.

Cess, R., et al., Absorption of solar radiation by clouds: Observations versus models, *Nature*, *267*, 496–499, 1995.

Chandrasekhar, S., *Radiative Transfer*, Oxford Univ. Press, New York, 1950.

Dahlback, A., Measurement of biologically effective UV doses, total ozone abundances, and cloud effects with multichannel, moderate bandwidth filter instruments, *Appl. Opt.*, *35*, 6514–6521, 1996.

Dianov-Klokov, V. I., and L. D. Krasnokutskaya, Comparison of observed and calculated effective photon path length in clouds, *Izv. Acad. Sci. USSR, Atmos. Oceanic Phys., Engl. Transl.*, *8*, 843–852, 1972.

Dobson, G. M. B., and C. W. B. Normand, Determination of the constants etc. used in the calculation of the amount of ozone from spectrophotometer measurements and of the accuracy of the results, *Ann. Int. Geophys. Year*, XVI, Part II, 161-191, Pergamon, London, 1962.

Elterman, L., UV, visible, and IR attenuation for altitudes to 50 km, AFCRL-68-0153 ERP 285, Air Force Cambridge Res. Lab., Bedford, Mass., 1968.

Erle, F., K. Pfeilsticker, and U. Platt, On the influence of tropospheric clouds on zenith–scattered–light measurements of stratospheric species, *Geophys. Res. Lett.*, *22*, 2725–2728, 1995.

Feigelson, E. M., *Radiation in a Cloudy Atmosphere*, D. Reidel, Norwell, Mass., 1984.

Fioletov, V., J. Kerr, and D. Wardle, The relationship between total ozone and spectral UV irradiance from Brewer observations and its use for derivation of total ozone from UV measurements, *Geophys. Res. Lett.*, *24*, 2997–3000, 1997.

Frederick, J. E., and D. Lubin, The budget of biologically active ultraviolet radiation in the earth-atmosphere system, *J. Geophys. Res.*, *93*, 3825–3832, 1988.

Frederick, J. E., P. F. Soulen, S. B. Diaz, I. Smolskaia, C. R. Booth, T. Lucas, and D. Neuschuler, Solar ultraviolet irradiance observed from southern Argentina: September 1990 to March 1991, *J. Geophys. Res.*, *98*, 8891–8897, 1993.

Gardiner, B., and P. Kirsch, Setting standards for european ultraviolet spectroradiometers, Report to the Commission of the European Communities, Contract STEP CT900076, Brussels, Belgium, 1995.

Grainger, J. F., and J. Ring, Anomalous fraunhofer line profiles, *Nature*, *193*, 762, 1962.

Hansen, J., Exact and approximate solutions for multiple scattering by cloudy and hazy planetary atmospheres, *J. Atmos. Sci.*, *26*, 478–487, 1969.

Høiskar, B. A. K., A. Dahlback, C. Tellefsen, and G. O. Braathen, Retrieval of total ozone abundances from the ultraviolet region of spectra recorded with an ultraviolet–visible spectrometer, *Appl. Opt.*, *36*, 7984–7991, 1997.

Hu, Y. X., and K. Stamnes, An accurate parameterization of the radiative properties of water clouds suitable for use in climate models, *J. Climate*, *6*, 728–742, 1993.

Joiner, J., P. K. Bhartia, R. P. Cebula, E. Hilsenrath, R. D. McPeters, and H. Park, Rotational–raman scattering (ring effect) in satellite backscatter ultraviolet measurements, *Appl. Opt.*, *34*, 4513–4525, 1995.

Kargin, B. A., L. D. Krasnokutskaya, and E. M. Feigelson,

Reflection and absorption of solar radiant energy by cloud layers, *Izv. Acad. Sci. USSR, Atmos. Oceanic Phys., Engl. Transl.*, *8*, 505–517, 1972.

Kurosu, T., V. V. Rozanov, and J. P. Burrows, Parameterization schemes for terrestrial water clouds in the radiative transfer model GOMETRAN, *J. Geophys. Res.*, *102*, 21,809–21,823, 1997.

Kylling, A., A. Albold, and G. Seckmeyer, Transmittance of a cloud is wavelength–dependent in the UV–range: Physical interpretation, *Geophys. Res. Lett.*, *24*, 397–400, 1997.

Lacis, A., J. Chowdhary, M. Mishchenko, and B. Cairns, Modeling errors in diffuse-sky radiation: Vector vs. scalar treatment, *Geophys. Res. Lett.*, *25*, 135–138, 1998.

Liou, K. N., *Radiation and Cloud Processes in the Atmosphere: Theory, Observation and Modeling*, Oxford Univ. Press, New York, 1992.

Madronich, S., UV radiation in the natural and perturbed atmosphere, in *Environmental Effects of UV (Ultraviolet) Radiation*, pp. 17–69, CRC Press, Boca Raton, 1993.

Mayer, B., and G. Seckmeyer, Retrieving ozone columns from spectral direct and global UV irradiance measurements, paper presented at XVIII Quadrennial Ozone Symposium, L'Aquila, Int. Assoc. for Meteorol. and Atmos. Sci., L'Aquila, Italy, 1996.

Mayer, B., G. Seckmeyer, and A. Kylling, Systematic long–term comparison of spectral UV measurements and UVSPEC modeling results, *J. Geophys. Res.*, *102*, 8755–8767, 1997.

Molina, L. T., and M. J. Molina, Absolute absorption cross sections of ozone in the 185– to 350–nm wavelength range, *J. Geophys. Res.*, *91*, 14,501–14,508, 1986.

Parzen, E., *Modern Probability Theory and Its Applications*, John Wiley, New York, 1960.

Pfeilsticker, K., F. Erle, and U. Platt, Absorption of solar radiation by atmospheric O_4, *J. Atmos. Sci.*, *54*, 934–939, 1997.

Plass, G. N., and G. W. Kattawar, Monte carlo calculations of light scattering from clouds, *Appl. Opt.*, *7*, 415–419, 1968.

Ridley, B. A., J. E. Dye, J. G. Walega, J. Zheng, F. E. Grahek, and W. Rison, On the production of active nitrogen by thunderstorms over New Mexico, *J. Geophys. Res.*, *101*, 20,985–21,005, 1996.

Seckmeyer, G., and G. Bernhard, Cosine error correction of spectral UV irradiances, in *Atmospheric Radiation* vol. 2049, edited by K. Stamnes, pp. 140–151, Int. Soc. for Opt. Eng., Bellingham, Wash., 1993.

Seckmeyer, G., et al., First intercomparison of spectral UV-radiation measurement systems, *Appl. Opt.*, *33*, 7805–7812, 1994.

Seckmeyer, G., et al., Geographical differences in the UV measured by intercompared spectroradiometers, *Geophys. Res. Lett.*, *22*, 1889–1892, 1995.

Seckmeyer, G., G. Bernhard, B. Mayer, and R. Erb, High–accuracy spectroradiometry of solar ultraviolet radiation, *Metrologia*, *32*, 697–700, 1996a.

Seckmeyer, G., R. Erb, and A. Albold, Transmittance of a cloud is wavelength–dependent in the UV–range, *Geophys. Res. Lett.*, *23*, 2753–2755, 1996b.

Stamnes, K., S.-C. Tsay, W. Wiscombe, and K. Jayaweera, Numerically stable algorithm for discrete–ordinate–method radiative transfer in multiple scattering and emitting layered media, *Appl. Opt.*, *27*, 2502–2509, 1988.

Stamnes, K., S. Pegau, and J. Frederick, Uncertainties in total ozone amounts inferred from zenith sky observations: Implications for ozone trend analyses, *J. Geophys. Res.*, *95*, 16,523–16,528, 1990.

Stamnes, K., J. Slusser, and M. Bowen, Derivation of total ozone abundance and cloud effects from spectral irradiance measurements, *Appl. Opt.*, *30*, 4418–4426, 1991.

van de Hulst, H. C., *Radiation and Cloud Processes in the Atmosphere: Theory, Observation and Modeling, Multiple Light Scattering*, vol. 2, Academic, San Diego, 1980.

Wang, P., and J. Lenoble, Influence of clouds on UV irradiance at ground level and backscattered exittance, *Adv. Atmos. Sci.*, *13*, 217–228, 1996.

Webb, A. R., Spectral measurements of solar ultraviolet-B radiation in southeast england, *J. Appl. Met.*, *31*, 212–216, 1992.

A. Kylling, Norwegian Institute for Air Research (NILU), N-9005 Tromsø, Norway. (e-mail: arve.kylling@nilu.no)

S. Madronich and B. Mayer, National Center for Atmospheric Research (NCAR), P.O. Box 3000, Boulder, CO 80307. (e-mail: sasha@ucar.edu, bmayer@ucar.edu)

G. Seckmeyer, Fraunhofer Institute for Atmospheric Environmental Research (IFU), Kreuzeckbahnstrasse 19, D-82467 Garmisch–Partenkirchen, Germany. (e-mail: seckmeyer@ifu.fhg.de)

(Received April 14, 1998; revised August 6, 1998; accepted August 10, 1998.)